Bifurcation Analysis of Switched Dynamical Systems With Periodically Moving Borders

Yue Ma, Hiroshi Kawakami, *Member, IEEE*, and Chi K. Tse, *Senior Member, IEEE*

***Abstract*—This paper describes a method for analyzing the bifurcation phenomena in switched dynamical systems whose switching borders are varying periodically with time. The type of systems under study covers most of power electronics circuits where two or more dynamical systems are cyclically switched according to the interaction of the state variables and some periodically moving borders. In particular, the complex bifurcation behavior of a voltage feedback buck converter is studied in detail. The analytical method developed in this paper allows bifurcation scenarios to be clearly revealed in any chosen parameter space.**

***Index Terms*—Bifurcation, border collision, buck converter, moving border, switched dynamical system, switching converter.**

I. Introduction

SWITCHED dynamical systems are useful in a variety of engineering applications. In electrical engineering, switched dynamical systems are found in sampled-data filters, oscillators, power converters, chaos generators, etc. Typically, a switched dynamical system operates by toggling among two or more dynamical systems according to a set of switching rules [1]. From an analytical viewpoint, we may look at a switched dynamical system as a set of two or more dynamical systems, each of which defines the system in a finite interval of time. Switching between one dynamical system to another occurs on a set of borders, which are defined on the system's state space. When the state variables cross the borders, appropriate switchings occur to re-define the dynamical flow. In a previous study by Kousaka *et al.* [2], switched dynamical systems with fixed borders are analyzed. Such systems, with fixed borders, can be considered as autonomous systems since switchings are determined only by the states of the system and are not affected by external signals. In many engineering applications, however, switchings are determined by the interaction of the states of the system with some external driving signal. Such an operation is found in most of power electronics circuits [3], [4], where the switching borders are defined by a periodic driving signal. Switched dynamical systems with moving borders are therefore nonautonomous. In this paper, we extend the work of Kousaka *et al.* [2] to the analysis of switched dynamical systems with their switching borders moving as functions of time.

Manuscript received March 19, 2003; revised October 18, 2003. This paper was recommended by Associate Editor M. Gilli.

Y. Ma and H. Kawakami are with the Department of Electrical and Electronic Engineering, University of Tokushima, Tokushima 770 8506, Japan. (e-mail: mayue@ee.tokushima-u.ac.jp)

C. K. Tse is with the Department of Electronic and Information Engineering, Hong Kong Polytechnic University, Hong Kong, China. (e-mail: encktse@polyu.edu.hk)

Digital Object Identifier 10.1109/TCSI.2004.829240

Being a characteristic phenomenon in switched dynamical systems, border collision bifurcation has attracted a lot of attention in recent years. Many researchers have studied border collision using the method of "normal form" [5]–[8], which effectively reduces a piecewise smooth map to a normal form in a small neighborhood of the border by a change of coordinates. Also, some consider border collision as "discontinuous bifurcation" which is caused by a jump of eigenvalues [9]. Since these approaches focus only on the neighborhood of the border, they are *local theory* of nonlinear dynamical systems. To get the normal form, one must know the trace and the determinant of the Jacobian matrix associated with the fixed point on each side of the border. These elements, however, bear no direct relevance to the practical system parameters with which engineers are most concerned. Thus, no general method for plotting bifurcation diagrams on the system parameter space has been presented. To solve these problems, we consider rather the global behavior of a periodic solution than the border's neighborhood. We construct analytical conditions for border collision and other bifurcations of specific periodic solutions. By examining these conditions in conjunction with the stability condition, we can identify the occurrence of various bifurcations in terms of the system parameters.

In much of the previous work, the Poincaré map, which has been defined in terms of duty cycle, has been found incapable in dealing with cases where multiple switchings occur in a periodic cycle [10], [11]. This is due to the particular (but unfortunately popular) way in which the Poincaré map was defined for switching systems. In this paper, we will define the Poincaré map in terms of the solution trajectory and border periodicity. We will see that the validity of the Poincaré map defined in this way can be extended to multiple-crossing cases.

We will first present a formal system description and a general procedure for analyzing the bifurcation behavior. To illustrate the practicality of the method, we apply the analysis procedure to a popular voltage feedback buck converter. We will show that bifurcation scenarios under the variation of any parameter can be uncovered by this method. In this paper, we systematically describe the bifurcation phenomena in the voltage feedback buck converter, covering the standard period-doubling [12], [13], saddle-node bifurcation as well as border collision bifurcation [6], [14]–[16]. We will show, from a practical perspective, how the operating regime of such a converter can be affected by the choice of parameters. In particular, the method we develop in this paper permits the types of bifurcations to be clearly and conveniently identified under different choices of parameter values. Hence, the results from the analysis can be

used by engineers to develop practically useful design rules for avoiding certain types of bifurcation scenarios.

II. System Formulation

A. Switched Dynamical Systems With Moving Borders

We begin our discussion by defining the type of systems we study in this paper. Consider two dynamical systems S_1 and S_2

$$\begin{aligned} S_1:\ \frac{\mathrm{d}x}{\mathrm{d}t} &= f(x,\lambda_1), \qquad x \in R^n \\ S_2:\ \frac{\mathrm{d}x}{\mathrm{d}t} &= g(x,\lambda_2), \qquad x \in R^n \end{aligned} \tag{1}$$

where λ_1 and λ_2 are the system parameters with appropriate dimensions. Next, we define a border B

$$B = \{x \in R^n :\ \beta(x,\, t) = 0\} \tag{2}$$

where $\beta(.)$ is a time-varying periodic function of period T, i.e.,

$$\beta(x, t+T) = \beta(x,\, t) \qquad \forall x \in B \qquad \forall t \in R.$$

This border B thus divides the state space into two parts, namely, M_1 and M_2, which are given by

$$\begin{aligned} M_1 &= \{(x,\, t) \in R^n \times R :\ \beta(x,\, t) \geq 0\} \\ M_2 &= \{(x,\, t) \in R^n \times R :\ \beta(x,\, t) \leq 0\}. \end{aligned} \tag{3}$$

The solution of the system in M_1 and M_2 is governed by the state equation corresponding to S_1 and S_2, respectively, as given in (1). Suppose the solutions in M_1 and M_2 are given by

$$\begin{aligned} x(t) &= \varphi(t, x_{01}) \quad x(0) = x_{01}, \qquad (x,\, t) \in M_1 \\ x(t) &= \psi(t, x_{02}) \quad x(0) = x_{02}, \qquad (x,\, t) \in M_2 \end{aligned} \tag{4}$$

where x_{01} and x_{02} are initial points located in M_1 and M_2, respectively.

Whenever the flow intersects the border B transversally, the system switches from S_1 to S_2, or vice versa. The point where the flow crosses the border can then be regarded as the initial point of the successive flow. Thus, we can describe any trajectory of this periodically switched system using the state equations of S_1 and S_2 in conjunction with the switching conditions defined by the border crossings.

B. Buck Converter

The foregoing system formulation indeed applies to many practical electronic circuits. Numerous examples can be found in power electronics. In particular, let us consider the voltage feedback buck converter shown in Fig. 1, which is a very popular circuit for stepping down dc voltages. In this circuit, switch S is controlled by a voltage comparator which compares a control signal $v_{\mathrm{con}}(t)$ with a ramp signal $V_{\mathrm{ramp}}(t)$. Essentially, switch S is open if $v_{\mathrm{con}}(t) > V_{\mathrm{ramp}}(t)$, and is closed otherwise. Here, v_{con} is derived from the output voltage through a standard error amplifier configuration. For simplicity, we consider a simple proportional type of feedback, as shown in Fig. 1. In this case, the control voltage can be written as

$$v_{\mathrm{con}}(t) = a(v_C(t) - V_{\mathrm{ref}}) \tag{5}$$

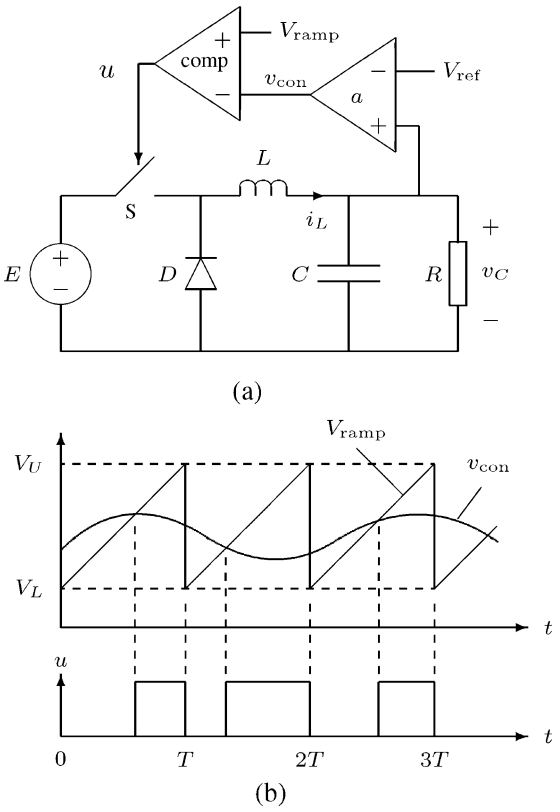

Fig. 1. Voltage feedback buck converter. (a) Schematic diagram. (b) Typical operating waveforms.

where a is the feedback amplifier gain. Also, the ramp signal is

$$V_{\mathrm{ramp}}(t) = V_L + (V_U - V_L)\frac{t}{T} \quad t \in [0, T]. \tag{6}$$

Therefore, the border function is given by

$$\begin{aligned} \beta(x,\, t) &= v_{\mathrm{con}}(t) - V_{\mathrm{ramp}}(t) \\ &= a\, v_C(t) - (V_U - V_L)\frac{t}{T} - aV_{\mathrm{ref}} - V_L \\ &= 0 \quad \text{for } t \in [0, T]. \end{aligned} \tag{7}$$

Now, the switching of S can be regarded as border crossing, and we may formulate this buck converter as

$$\begin{aligned} S_1:\ \frac{\mathrm{d}x}{\mathrm{d}t} &= Ax, \qquad \beta(x,\, t) \geq 0 \\ S_2:\ \frac{\mathrm{d}x}{\mathrm{d}t} &= Ax + BE, \qquad \beta(x,\, t) \leq 0 \end{aligned} \tag{8}$$

where

$$x = \begin{bmatrix} v_C \\ i_L \end{bmatrix} \quad A = \begin{bmatrix} -\frac{1}{RC} & \frac{1}{C} \\ -\frac{1}{L} & 0 \end{bmatrix} \quad B = \begin{bmatrix} 0 \\ \frac{1}{L} \end{bmatrix}. \tag{9}$$

Since the border function $\beta(x,\, t)$ is independent of i_L, the border manifold B is parallel to the direction of i_L in the 2-dim phase plane, as shown in Fig. 2(a). The dynamics above the border is governed by the state equation of S_1, and that below the border is governed by the state equation of S_2. Meanwhile, the border moves in the vertical direction within a specific region periodically. The movement is defined by (7), which is depicted by the ramp signal shown in Fig. 2(b). Note that a latch is often used in the practical control loop to avoid multiple crossings in one cycle. Here, we omit the latch in order to consider

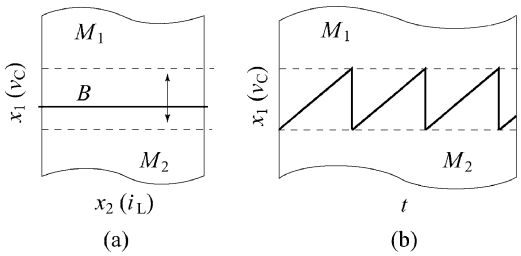

Fig. 2. Periodically moving border in the buck converter.

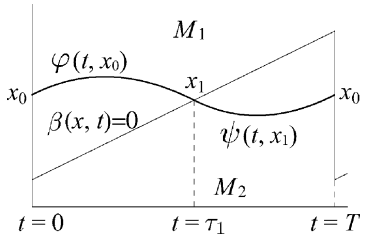

Fig. 3. Period-1 solution in the buck converter denoted as P1(1).

a more general example of switched dynamical systems satisfying the definition of Section II-A.

From the above description, we can see that the voltage feedback buck converter is a switched dynamical system with periodically moving border. We will use this model to illustrate our solution approach.

III. Poincaré Map and Periodic Solutions

Since the border movement is periodic, we can conveniently define the Poincaré map F as follows:

$$F:\ R^n \to R^n \quad x(0) \mapsto x(T). \tag{10}$$

This straightforward definition gives the Poincaré map the capability to describe arbitrary trajectory between 0 and T. Based on the formulation described in Section II-A, any solution can be constructed according to the initial conditions and switching actions. In particular, if a solution satisfies

$$x(0) = x(kT), \qquad k = 1, 2, \ldots \tag{11}$$

it is a period-k solution, i.e., the solution is invariant under the map F^k.

For notational clarity, we will denote periodic solutions as $\mathrm{P}n(k_1, k_2, \ldots, k_n)$, where n is the period of the solution and $k_1, k_2, \ldots, k_n$ indicates the number of times the solution crosses the border in each period. For example, the solution shown in Fig. 3 is denoted as P1(1). This solution is the simplest periodic solution for the buck converter, and is often the preferred operating regime for most practical applications. Likewise, P2(0,1) denotes a period-2 solution with no border crossing in the first period and one border crossing in the second period, etc.

With the solution and border function given by (4) and (7), we can then take the following steps to find the periodic solution. We refer to Fig. 3 for ease of description.

1) In the first interval $0 \le t \le \tau_1$, i.e., $(x, t) \in M_1$, we have

$$x_1 = \varphi(\tau_1, x_0). \tag{12}$$

2) At $t = \tau_1$, we put x_1 as the initial point for the flow during $\tau_1 \le t \le T$, i.e., $(x, t) \in M_2$. Then, enforcing the boundary condition, we have

$$x_0 = \psi(T - \tau_1, x_1). \tag{13}$$

3) Moreover, the border crossing condition is

$$\beta(x_1, \tau_1) = 0. \tag{14}$$

Clearly, (12), (13), and (14) contain five scalar equations from which the five scalar unknowns x_0, x_1, and τ_1 can be solved using an appropriate numerical method.

IV. Classification of Bifurcations and Analysis Methods

Like many nonlinear systems, switched dynamical systems can exhibit a rich variety of bifurcation behavior. Generally speaking, if the phase portrait changes its topological structure as a parameter is varied, the system is said to undergo a bifurcation [17], [18]. Most standard types of bifurcations are caused by the loss of stability of a solution and the picking up of another. For switched dynamical systems, moreover, a special type of bifurcation, known as border collision, is often observed. This type of bifurcation is not caused by a loss of stability of the solution, but by a change in the system operation [4]. In the following, we will discuss these bifurcations and their interplay in detail.

A. Standard Bifurcation From Change of Stability Status

The stability of a periodic solution can be determined by calculating the eigenvalues of the linearized system around the fixed point. For example, if one eigenvalue passes through -1 as a parameter is varied, the solution undergoes a *period-doubling bifurcation*. Also, if one eigenvalue is equal to $+1$ as a parameter is varied, the solution undergoes a *saddle-node bifurcation*, etc. [17], [18]. These types of bifurcation have been widely studied and are often considered as standard types of bifurcation in nonlinear systems. In the following, we describe a general procedure for analyzing these bifurcations, which is applicable to any switched dynamical system.

Let us take the period-1 solution discussed in Section III as an example. To get the linearized system at the fixed point x_0, we consider the trajectory at $t = \tau_1$ and $t = T$, denoted by x_1 and x_2, respectively

$$x_1 = \varphi(\tau_1, x_0) \tag{15}$$

$$x_2 = \psi(T - \tau_1, x_1) \tag{16}$$

$$\beta(x_1, \tau_1) = 0. \tag{17}$$

Note that the Poincaré map in this case is simply the function $\psi(T - \tau_1, \varphi(\tau_1, x))$. Here, we are interested in the linearized dynamics near the small neighborhood of x_0, which can be simply described by $\partial x_2/\partial x_0$, i.e., the Jacobian of the Poincaré map.

From (15) and (16), we get

$$\frac{\partial x_2}{\partial x_0} = \frac{\partial \psi}{\partial t}\left(-\frac{\partial \tau_1}{\partial x_0}\right) + \frac{\partial \psi}{\partial x_1}\frac{\partial x_1}{\partial x_0} \tag{18}$$

$$\frac{\partial x_1}{\partial x_0} = \frac{\partial \varphi}{\partial t}\frac{\partial \tau_1}{\partial x_0} + \frac{\partial \varphi}{\partial x_0} \tag{19}$$

where φ and ψ denote $\varphi(\tau_1, x_0)$ and $\psi(T-\tau_1, x_1)$, respectively. Note that the partial derivative of the crossing time, i.e., $\partial\tau_1/\partial x_0$, must be considered in the above equations. From (17), we have

$$\begin{aligned}\frac{\partial\beta}{\partial x_0} &= \frac{\partial\beta}{\partial x}\frac{\partial x_1}{\partial x_0} + \frac{\partial\beta}{\partial t}\frac{\partial\tau_1}{\partial x_0} \\ &= \frac{\partial\beta}{\partial x}\left(\frac{\partial\varphi}{\partial t}\frac{\partial\tau_1}{\partial x_0} + \frac{\partial\varphi}{\partial x_0}\right) + \frac{\partial\beta}{\partial t}\frac{\partial\tau_1}{\partial x_0} \\ &= 0. \end{aligned} \tag{20}$$

Hence, $\partial\tau_1/\partial x_0$ can be obtained as

$$\frac{\partial\tau_1}{\partial x_0} = -\frac{1}{\frac{\partial\beta}{\partial x}\frac{\partial\varphi}{\partial t} + \frac{\partial\beta}{\partial t}}\frac{\partial\beta}{\partial x}\frac{\partial\varphi}{\partial x_0}. \tag{21}$$

Then, by writing $\partial\varphi/\partial t$ and $\partial\psi/\partial t$ as $f(\varphi)$ and $g(\psi)$, and putting (19) and (21) in (18), we get

$$\begin{aligned}\frac{\partial x_2}{\partial x_0} = &\frac{\partial\psi}{\partial x_1}\frac{\partial\varphi}{\partial x_0} + \frac{1}{\frac{\partial\beta}{\partial x}f(\varphi) + \frac{\partial\beta}{\partial t}} \\ &\cdot\left(g(\psi) - \frac{\partial\psi}{\partial x_1}f(\varphi)\right)\frac{\partial\beta}{\partial x}\frac{\partial\varphi}{\partial x_0}\end{aligned} \tag{22}$$

where $\partial\varphi/\partial x_0$ and $\partial\psi/\partial x_1$ are solutions of the following differential equations:

$$\begin{cases} \frac{d}{dt}\left(\frac{\partial\varphi}{\partial x_0}\right) = \frac{\partial f}{\partial x}\left(\frac{\partial\varphi}{\partial x_0}\right), \\ \frac{d}{dt}\left(\frac{\partial\psi}{\partial x_1}\right) = \frac{\partial g}{\partial x}\left(\frac{\partial\psi}{\partial x_1}\right), \end{cases} \quad \left.\frac{\partial\varphi}{\partial x_0}, \frac{\partial\psi}{\partial x_1}\right|_{t=0} = I_n. \tag{23}$$

Thus, we can calculate the Jacobian of the Poincaré map by an appropriate numerical method. Finally, by finding the roots $\{\mu_1, \mu_2, \ldots, \mu_n\}$ of the characteristic equation

$$\left|\frac{\partial x_2}{\partial x_0} - \mu I_n\right| = 0 \tag{24}$$

we can determine the stability of the periodic solution and analyze the bifurcation behavior.

We should stress that the above procedure is completely general, without involving specific system definitions and border function. Also, it can be easily extended to systems that contain more than one border functions.

B. Border Collision From Change of Operation

Unlike the standard bifurcation behaviors which involve the change of stability status, border collision is a result of operational change which is commonly observed in switched dynamical systems where the usual switching sequence can be disrupted under certain conditions. Since the way in which operation changes is system dependent, we have to focus on a specific system in order to illustrate the method. In the following, we present an analysis, along with a classification of the possible operational changes, for the same buck converter system described earlier. Also, instead of using the normal form method [5]–[7], we will take on a global approach in our analysis.

When the switching sequence of a switched dynamical system is altered as a parameter is varied, the behavior may change abruptly and such a phenomenon is generally called border collision. For the buck converter under study, the basic cause for border collision is the natural saturation of the duty cycle, which is always bounded between 0 and 1. Referring to Fig. 1, $v_{\rm con}$ is limited from above by V_U as well as from below by V_L. When it hits the ramp voltage $V_{\rm ramp}$, switching action happens. Thus, at the point where $v_{\rm con}$ just leaves the allowable range, i.e., $v_{\rm con}$ "grazes" at the upper or lower tip of the ramp signal, the system is said to undergo a border collision.

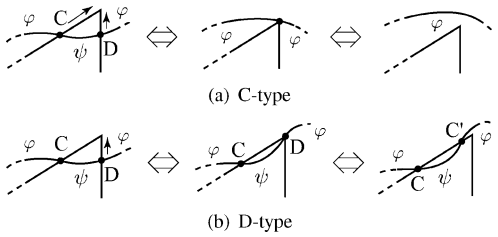

Fig. 4. Classification of border collision in buck converter.

We classify border collision in the buck converter into two types, as depicted in Fig. 4, according to the way in which $v_{\rm con}$ interacts with the ramp at the point of border collision. Consider the situation before a border collision takes place. Suppose C is the intersecting point of $v_{\rm con}$ with the ramp signal, and D is the point where $v_{\rm con}$ crosses the vertical edge of the ramp signal, as indicated in Fig. 4. After the border collision, we may identify two possible scenarios.

1) If both C and D move upward and conjoin at the vertex of the ramp, the type of border collision is classified as "C-type." See Fig. 4(a).
2) If only point D moves up and leaves the ramp from its vertex, creating a new intersection point C', the type of border collision is classified as "D-type." See Fig. 4(b).

Obviously, both scenarios can happen at the lower tip of the ramp, and we may, in principle, classify the corresponding scenarios as C-type and D-type.

Although the two types of border collision lead to different behavioral changes, they can be analyzed under a unified approach, as described in the following. First, we recognize that the condition for border collision is the "touching" of $v_{\rm con}$ with the upper tip of $V_{\rm ramp}$. A relevant equation can therefore be written to describe this condition. This new equation can be added to the earlier set of equations describing the periodic solution to form a new set of equations. Solving this, we can obtain the parameter condition under which a specific border collision occurs. An example will clarify this procedure.

Consider a border collision from a period-2 solution. The situation is shown in Fig. 5, where $\square$ denotes the grazing point. To find the value of E (input voltage) at which border collision occurs, we solve the following set of equations:

$$\begin{aligned} x_1 &= \varphi(T,\, x_0,\, E) \\ x_2 &= \varphi(\tau_2,\, x_1,\, E) \\ x_0 &= \psi(T-\tau_2,\, x_2,\, E) \\ \beta(x_1,\, T) &= 0 \qquad \text{(border collision 's condition)} \\ \beta(x_2,\, \tau_2) &= 0 \end{aligned} \tag{25}$$

where all symbols are defined earlier or explained in Fig. 5. We note that (25) contains eight scalar equations from which the eight scalar unknowns, x_0, x_1, x_2, τ_2, E, can be solved. Moreover, for a specific border collision, the operational sequence of

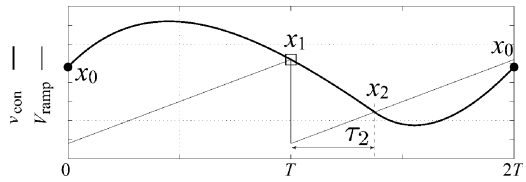

Fig. 5. Border collision (Bc2a) of period-2 solution.

TABLE I
SYSTEM OF ABBREVIATIONS OF BIFURCATION. EACH TYPE OF BIFURCATION IS ABBREVIATED AS $\triangle n \sharp$

$\triangle$	D	Period-doubling bifurcation
	S	Saddle-node bifurcation
	Bc	C-type border collision
	Bd	D-type border collision
n	1,2,$\cdots$	Period of solution to which bifurcation occurs
$\sharp$	a,b,$\cdots$	Index

the resulting solution after bifurcation is known. Then, by analyzing the stability of the resulting solution as introduced in Section IV, we can investigate how system behavior is altered by a border collision.

V. BIFURCATION BEHAVIOR OF BUCK CONVERTER

In this section, we will investigate the complicated bifurcation behavior exhibited by the buck converter described in Section II-B. To facilitate numerical analysis, we fix some of the parameters as follows:

$$L = 20\ \text{mH} \quad a = 8.4 \quad V_{\text{ref}} = 11.3\ \text{V}$$
$$V_L = 3.8\ \text{V} \quad V_U = 8.2\ \text{V} \quad \text{and} \quad T = 400\ \mu\text{s}.$$

Using the analysis methods developed in the foregoing section, together with appropriate numerical calculations, we can obtain bifurcation diagrams for any given ranges of parameters.

For the sake of clarity and to avoid confusion, we adopt a system for denoting the bifurcation curves on the bifurcation diagrams, as explained in Table I. For example, the period-doubling bifurcation from a period-1 solution to a period-2 solution is denoted as D1. Likewise, the period-doubling bifurcation from a period-2 solution to a period-4 solution is denoted as D2. But if there are two such bifurcations in different parameter regions, we denote them as D2a and D2b, etc.

A. Detailed Bifurcation Behavior of the Buck Converter

In practice, a converter is designed to work in a range of input voltage and output load resistance. It is therefore useful to examine the bifurcation behavior with the input voltage and load resistance serving as the bifurcation parameters, and with other circuit parameters fixed. Moreover, the inductance is usually dictated by the choice of operating mode and the required ripple level, whereas the output capacitance can be chosen according to the transient requirement. In our study, we will keep the inductance fixed, and consider the bifurcation behavior for different choices of the output capacitance.

We begin with $C = 47\ \mu$F, which is typical for the switching frequency concerned. A bifurcation diagram in the E–R plane and a blow-up view are shown in Fig. 6. From these diagrams,

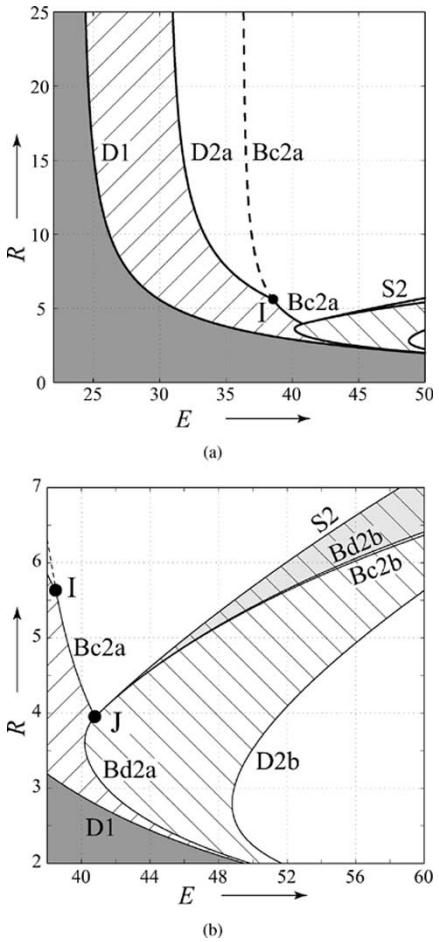

Fig. 6. (a) Bifurcation diagram in E–R plane with $C = 47\ \mu$F. (b) Enlarged view.

in conjunction with the waveforms shown in Figs. 7 and 8, we are able to make the following observations regarding the bifurcation behavior of period-1 and period-2 solutions.

1) In the dark-grey region [shown in Fig. 6(a)], the stable solution is P1(1) for which only period-doubling D1 is observed.
2) Period-2 solutions exhibit a much richer bifurcation behavior. In Fig. 7, we show the phase portraits and waveforms of some typical period-2 solutions. Here, for P2(1,1), a period-doubling D2a and border collision are possible, as shown in Fig. 6(a). Note that Bc2a is the situation depicted earlier in Fig. 5.
3) Some complex bifurcation behavior can be observed around point I on the bifurcation diagram. Crossing the bifurcation curve of Bc2a from left to right, P2(1,1) becomes P2(0,1), as depicted in Fig. 7(d). However, inspecting the eigenvalues of P2(0,1), we find that P2(0,1) is unstable.
4) Crossing the bifurcation curve of Bc2a from left to right above point I, we see that D2a takes place ahead of Bc2a. For clarity, Bc2a happening on unstable solution P2(1,1) is shown as a dashed curve in Fig. 6(a).
5) From the blow-up view of Fig. 6(b), we observe that another border collision Bd2a occurs below point J. This bifurcation, corresponding to Fig. 8(a), transmutes

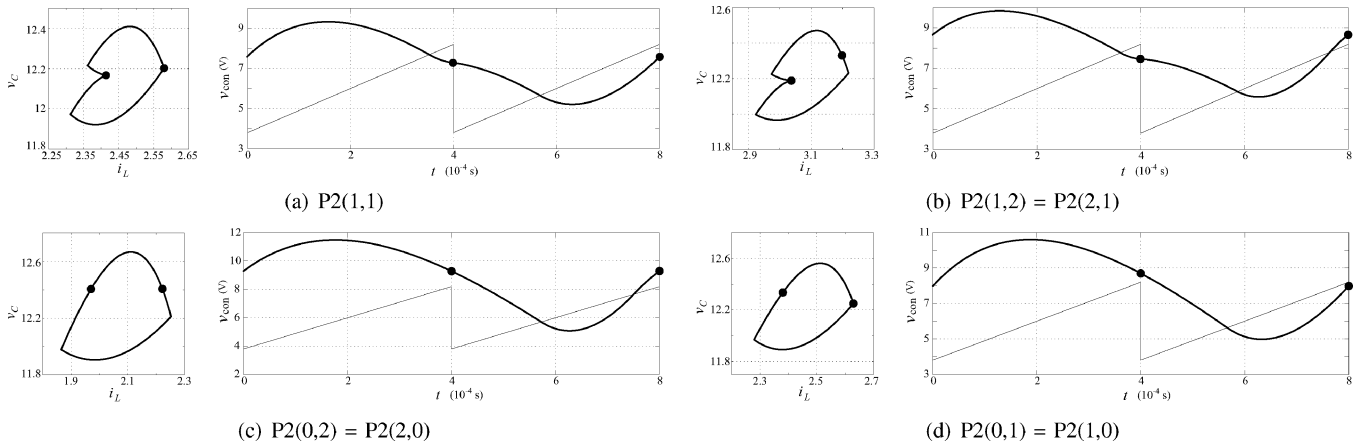

Fig. 7. Phase portraits and waveforms of $v_{\rm con}$ and $V_{\rm ramp}$ for some typical period-2 solutions.

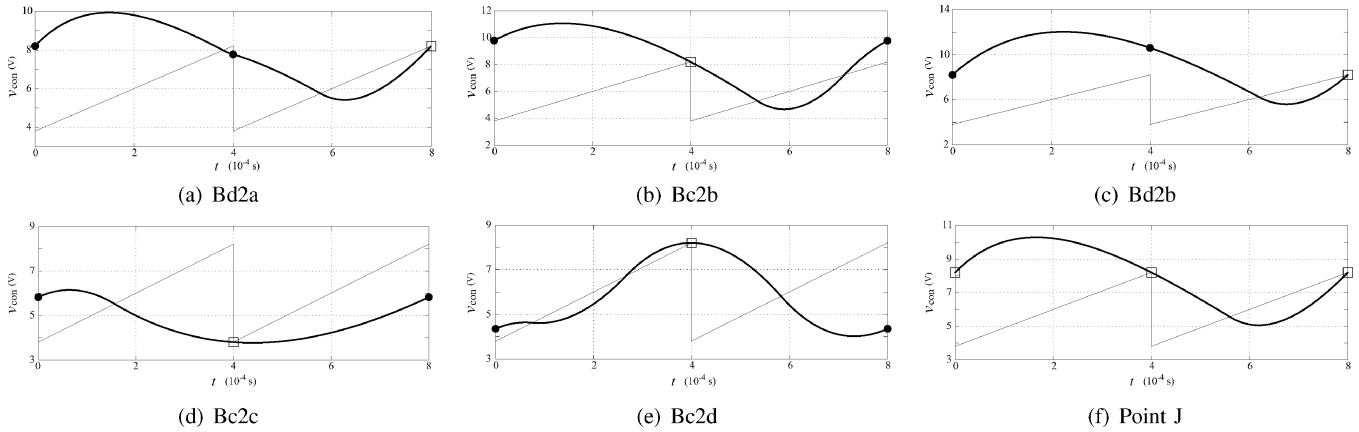

Fig. 8. Conditions of various border collision bifurcations. □ indicates grazing point.

P2(1,1) into P2(1,2). Note that P2(1,2) is a stable period-2 solution as shown in Fig. 7(b). Also, P2(1,2) can undergo period-doubling and saddle-node bifurcation, denoted as D2b and S2 respectively on the bifurcation diagrams. For ease of reference, the region in which P2(1,1) exists is shown as the hatched area, and the region in which P2(1,2) exists is shown as the back-hatched area.

6) As mentioned above, P2(0,1) is unstable. This unstable P2(0,1) undergoes another border collision Bd2b to become P2(0,2), as depicted in Fig. 8(c). The solution P2(0,2), corresponding to Fig. 7(c), is stable and only exists in a narrow region between Bd2b and Bc2b.
7) Since P2(0,1) is unstable, the Bc2a discussed earlier actually leads to P4(0,1,1,1). Moreover, chaotic state appears in succession. That is, P2(0,1), as a periodic solution, is never manifested. Thus, in the light-gray region [shown in Fig. 6(b)], we actually find a stable period-2 solution coexisting with possible longer periodic solutions or chaos.
8) Bc2b, corresponding to Fig. 8(b), transmutes P2(0,2) into P2(1,2).
9) Four border collision curves meet at the same point J on the bifurcation diagram. The coordinate of J is (40.781 V, 3.946 Ω). At this set of parameters, both C and D types of border collision occur at the same time. This situation is illustrated in Fig. 8(f).

B. Fundamental Differences Between C-Type and D-Type Border Collisions

We may obtain some specific bifurcation diagrams by fixing R at certain values. For instance, with $R = 3\ \Omega$ and 5.4 Ω, we obtain the bifurcation diagrams shown in Fig. 9. These diagrams are able to reveal further details of the bifurcation behavior. Specifically, we can see clearly from Figs. 9(c) and (d) the coexisting solutions. Furthermore, we observe an important difference in the manifestations of the C-type and D-type border collision on the bifurcation diagrams. *The C-type border collision manifests itself as a leap, whereas the D-type manifests as an inflection.* This difference can be attributed to the kind of operational change associated with the specific type of border collision. Specifically, in the C-type border collision, the switching sequence is disrupted, giving rise to "skipped" cycles. Moreover, in the D-type border collision, the relative durations of the on and off intervals are disturbed while the same switching sequence is maintained. Fig. 10 shows a schematic comparison between the two types of border collision. Thus, we expect a more severe alteration in the circuit operation due to a C-type border collision.

C. Effects of the Value of Output Capacitance

As mentioned earlier, the output capacitance can be chosen by the circuit designer to suit specific applications. Here, we are

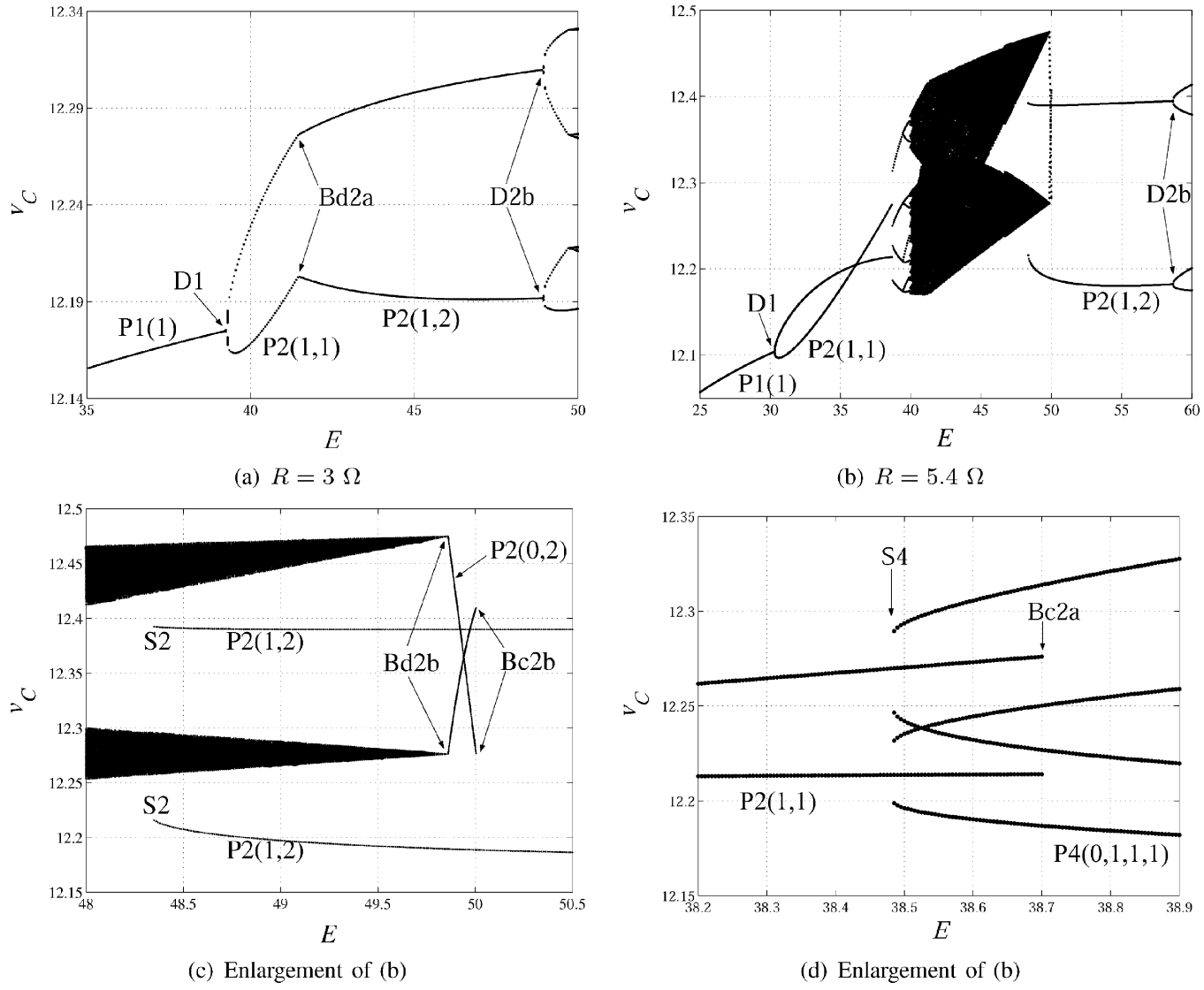

Fig. 9. Bifurcation diagrams for fixed R, with E serving as the bifurcation parameter.

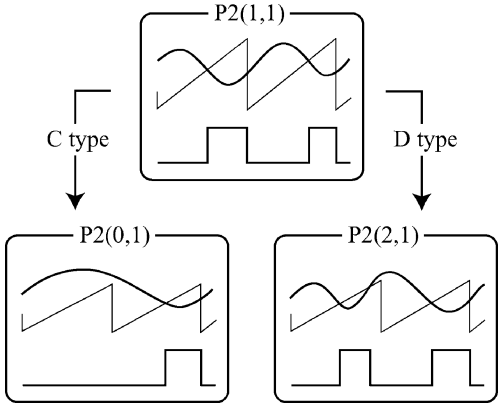

Fig. 10. Operational difference between C-type and D-type border collisions.

interested to see how the bifurcation behavior will be affected by the choice of the output capacitance value.

We consider the case with $C = 33\ \mu$F. The corresponding bifurcation diagram is shown in Fig. 11. In this case, we observe the same rich bifurcation behavior, but the locations of occurrence of the various bifurcations on the E–R plane differ significantly from those corresponding to the case of $C = 47\ \mu$F. A few observations are summarized as follows.

1) We begin with the familiar Bc2a, which is supposed to transmute P2(1,1) to P2(0,1). In this case, D2a always goes ahead of Bc2a. Thus, Bc2a transmutes unstable P2(1,1) to unstable P2(0,1). Again, we use a dashed curve to indicate this situation.
2) The region in which the stable P2(2,1) exists is much larger than the corresponding region for the case of $C = 47\ \mu$F.
3) In addition to D2b, P2(2,1) exhibits another period-doubling bifurcation as E decreases (i.e., from right to left), denoted as D2c in Fig. 11. This D2c is interrupted by Bc2d, which is depicted in Fig. 8(e). Also, Bc2d, crossing from right to left in Fig. 11, transmutes stable P2(2,1) into unstable P2(3,1).
4) Another border collision Bc2c is found. This bifurcation occurs for relatively small values of E, corresponding to

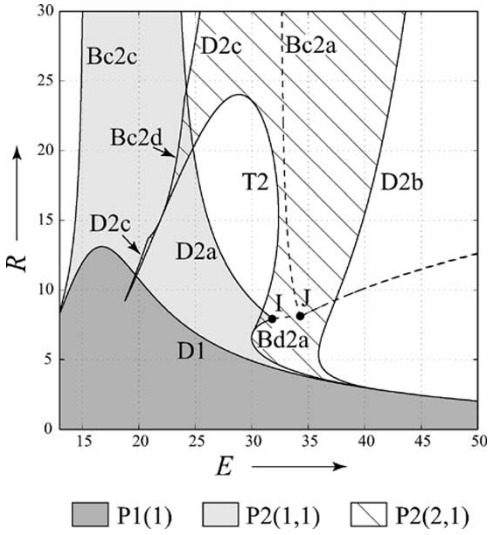

Fig. 11. Bifurcation diagram in E–R plane with $C = 33\ \mu$F.

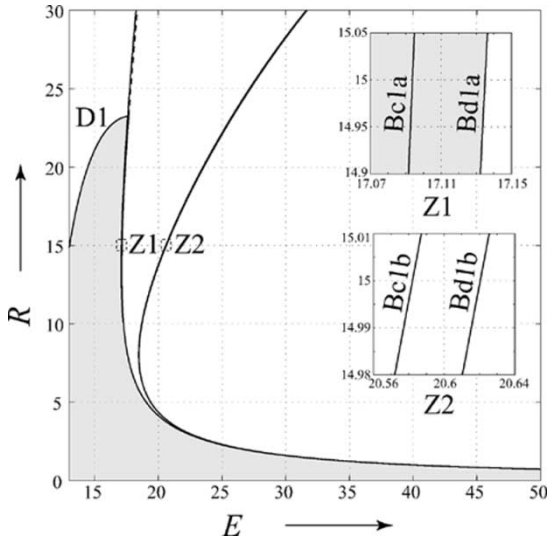

Fig. 12. Bifurcation diagram in E–R plane with $C = 4.7\ \mu$F.

the case where the control voltage hits the lower tip of the ramp signal. This situation is illustrated in Fig. 8(d). Moreover, solutions created by Bc2c, crossing from right to left in Fig. 11, are unstable.

Next, we consider an even smaller output capacitance. With $C = 4.7\ \mu$F, the converter responds much more rapidly and border crossing occurs more frequently. Here, in the absence of a latch in the circuit, we can see many multiple-crossing instances, and many border collision bifurcations associated with multiple-crossing are possible. The bifurcation diagram is presented in Fig. 12. We summarize a few key features as follows.

1) In the light-gray region (shown in Fig. 12), P1(1) solution exists. This P1(1) solution undergoes period-doubling D1 as well as border collision Bd1a.
2) Bc1a and Bd1a occur in close proximity, and so do Bc1b and Bd1b, as depicted in the enlargements Z1 and Z2 shown in Fig. 12. The situations corresponding to these period-1 border collisions are shown in Fig. 13.

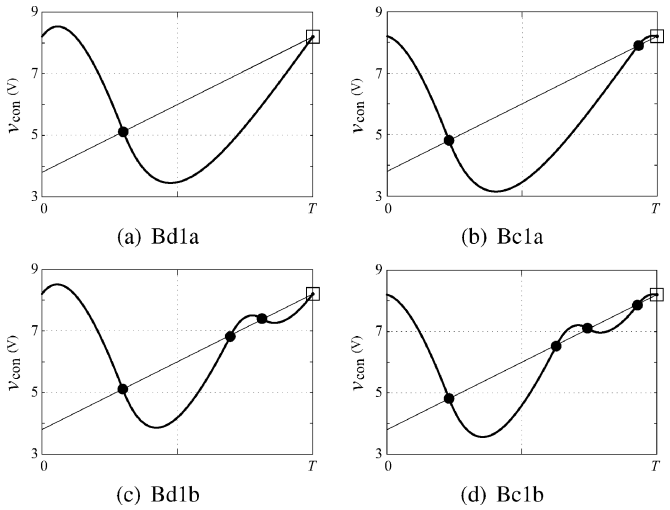

Fig. 13. Conditions of border collision in period-1 solutions.

3) Multiple-crossing solutions exist. For example, P1(3) exists between Bc1a and Bd1b, and Bc1b gives rise to P1(5).

Again, we take the liberty of fixing R at a certain value to reveal further details of the bifurcation behavior. For $R = 15\ \Omega$, we obtain a bifurcation diagram with E serving as the bifurcation parameter, as shown in Fig. 14(a). As E increases, border crossing becomes more and more frequent, as shown in Fig. 14(b). Furthermore, enlarging the bifurcation diagram near the cusps reveals some interesting behavior. For the first cusp, as shown in Fig. 14(c), an unstable P1(2) exists in a narrow range of E, whose endpoints are defined by the onset of Bc1a and Bd1a which connect P1(2) with P1(3) and P1(1). In summary, the bifurcation scenarios near the cusps involve generic border collision, although they may look deceptively like saddle-node bifurcations.

D. Interplay of Border Collision and Period-Doubling Bifurcation

As mentioned earlier, border collision can occur in unstable solutions. Such border collisions are normally unobserved and ignored in practice. However, as we will see shortly, border collisions of unstable solutions can provide useful clues for predicting the occurrence of chaos.

Without probing into the detailed mechanisms of the formation of chaotic attractors, we can intuitively explain (and estimate) the location of the onset of chaos in terms of an important behavior which is associated with the interplay between the main period-doubling cascade and border collisions. A schematic illustration is shown in Fig. 15. In the normal period-doubling bifurcation, a solution loses its stability and generates a solution whose period is doubled. In the period-doubling cascade, period-doubling bifurcation continues to generate solutions of longer periods and to chaos, as the parameter continues to vary in the chosen direction. However, border collision comes into play, for the class of systems under study, and interrupts the normal period-doubling cascade, as depicted in Fig. 15(a).

Generally speaking, whenever v_C hits a boundary, e.g., $v_C B$, border collision occurs. For the buck converter, if we focus on

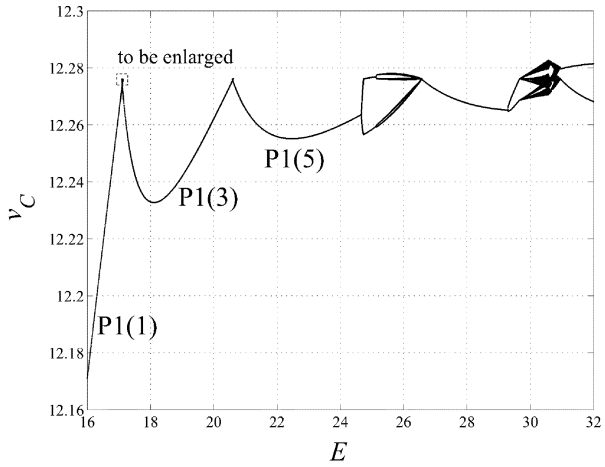

(a) Bifurcation diagram

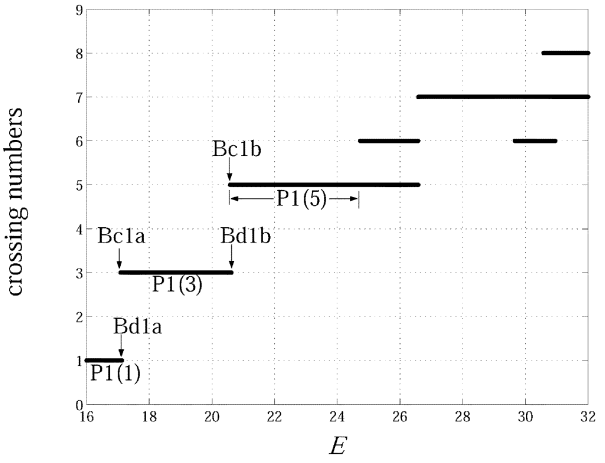

(b) Number of crossings

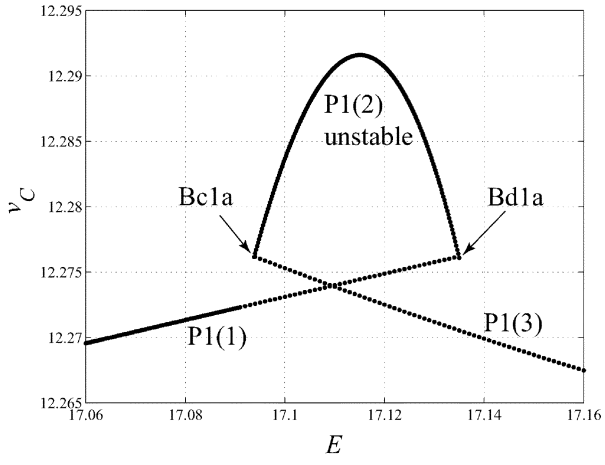

(c) Enlargement of (a)

Fig. 14. Bifurcation diagrams based on the Poincaré map with E serving as bifurcation parameter for $R = 15\ \Omega$ and $C = 4.7\ \mu$F.

the border collision associated with grazing of the control signal at the upper tip of the ramp signal, we have

$$v_C B = \frac{V_U}{a} + V_{\text{ref}}. \tag{26}$$

With this added feature, we see from Fig. 15(a) that the border collision of stable period-8 solution (**B8**) must happen before the border collision *B4* of the unstable period-4 solution and after

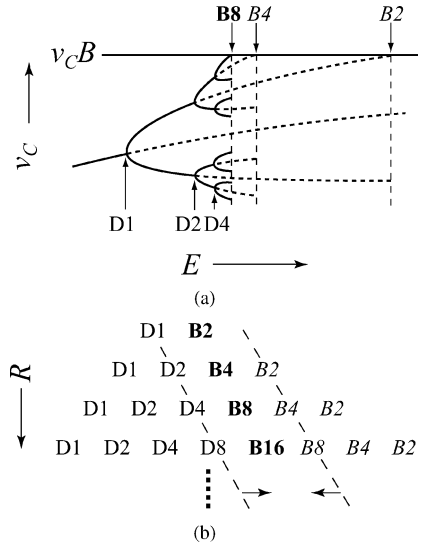

Fig. 15. (a) Schematic bifurcation diagram showing interplay between border collision and period-doubling cascade. (b) Typical bifurcation sequence.

the period-doubling D4 of the stable period-4 solution. The entire period-doubling cascade will move upward as R is reduced. Note that the vertical axis is v_C in Fig. 15(a). Thus, as R decreases, **B8** and D4 will soon be displaced from the top (disappear) while **B4** will occur for the stable period-4 solution.

In general, we may conceive a bifurcation pattern, as shown in Fig. 15(b), which illustrates the interplay between period-doubling bifurcations and border collisions. We now look at the bifurcation with E serving as the parameter and increasing. The first border collision (marked in boldface) must be located between a period-doubling of a stable solution and a border collision of an unstable solution (marked in italics), as depicted in Fig. 15(b). The region where the first border collision is hit becomes narrower and narrower as the period of the solution lengthens. Moreover, these first border collisions often represent overtures to prelude the occurrence of chaos. Referring to Fig. 15(a), we can conclude that chaos occurs between Bc2a and D2a. Here, point I can be interpreted as a critical point where the bifurcation sequence jumps from the second row to the first row in Fig. 15(b). However, we should stress that this simple rule, though helpful in making prediction of the onset of chaos, has assumed the validity of an ideal period-doubling cascade.

VI. Conclusion

In this paper, we have introduced a method for analyzing the bifurcation behavior of switched dynamical systems with periodically moving borders. By constructing the periodic solutions according to the switching sequences, we can find periodic orbits, evaluate their stability, and study the bifurcation behavior. The method developed in this paper leads to the plotting of detailed bifurcation diagrams on the parameter space that can provide useful practical information for engineers to determine the complex bifurcation behavior of any given switched dynamical system. In particular, we have provided specific bifurcation diagrams for the voltage feedback buck converter and discussed the key features of the bifurcation behavior. In this paper we have limited ourselves to the study of bifurcations of period-1

and period-2 solutions. We have shown the rich variety of possible border collision scenarios and their interplay with the main period-doubling cascade. The same method of analysis can be extended to solutions of longer periods, with higher complexity of the numerical solution being the price to pay.

REFERENCES

[1] T. Kousaka, T. Ueta, and H. Kawakami, "Chaos and control of periodically switched nonlinear systems," *Latin Amer. Appl. Res.*, vol. 31, pp. 211–218, Sept. 2001.

[2] ——, "Bifurcation of switched nonlinear dynamical systems," *IEEE Trans. Circuits Syst. II*, vol. 46, pp. 878–885, July 1999.

[3] S. Banerjee and G. Verghese, Eds., *Nonlinear Phenomena in Power Electronics: Attractors, Bifurcations, Chaos, and Nonlinear Control*. New York: IEEE Press, 2001.

[4] C. K. Tse, *Complex Behavior of Switching Power Converters*. Boca Raton, FL: CRC, 2003.

[5] H. E. Nusse and J. A. Yorke, "Border-collision bifurcations including 'period two to period three' for piecewise smooth systems," *Phys. D*, vol. 57, pp. 39–57, 1992.

[6] G. Yuan, S. Banerjee, E. Ott, and J. A. Yorke, "Border-collision bifurcation in the buck converter," *IEEE Trans. Circuits Syst. I*, vol. 45, pp. 707–716, July 1998.

[7] S. Banerjee, P. Ranjan, and C. Grebogi, "Bifurcation in two-dimensional piecewise smooth maps – Theory and applications in switching circuits," *IEEE Trans. Circuits Syst. I*, vol. 47, pp. 633–643, May 2000.

[8] M. di Bernardo, C. J. Budd, and A. R. Champneys, "Grazing and border-collision in piecewise-smooth systems: A unified analytical framework," *Phys. Rev. Lett.*, vol. 86, no. 12, pp. 2553–2556, 2001.

[9] R. I. Leine, D. H. V. Campen, and B. L. V. de Vrande, "Bifurcations in nonlinear discontinuous systems," *Nonlin. Dyn.*, vol. 23, pp. 105–164, 2000.

[10] E. Fossas and G. Olivar, "Study of chaos in the buck converter," *IEEE Trans. Circuits Syst. I*, vol. 43, pp. 13–25, Jan. 1996.

[11] M. di Bernardo, F. Garofalo, L. Glielmo, and F. Vasca, "Switchings, bifurcations, and chaos in dc/dc converters," *IEEE Trans. Circuits Syst. I*, vol. 45, pp. 133–141, Feb. 1998.

[12] J. H. B. Deane and D. C. Hamill, "Instability, subharmonics, and chaos in power electronic circuits," *IEEE Trans. Power Electron.*, vol. 5, pp. 260–268, July 1990.

[13] D. C. Hamill, J. H. B. Deane, and D. J. Jefferies, "Modeling of chaotic dc/dc converters by iterative nonlinear mappings," *IEEE Trans. Power Electron.*, vol. 7, pp. 25–36, Jan. 1992.

[14] M. di Bernardo, E. Fossas, G. Olivar, and F. Vasca, "Secondary bifurcations and high-periodic orbits in voltage controlled buck converter," *Int. J. Bifurcation Chaos*, vol. 12, no. 7, pp. 2755–2771, 1997.

[15] H. E. Nusse, E. Ott, and J. A. Yorke, "Border-collision bifurcations: An explanation for observed bifurcation phenomena," *Phys. Rev. E*, vol. 49, pp. 1073–1076, 1994.

[16] Z. T. Zhusubaliyev, E. A. Soukhoterin, and E. Mosekilde, "Border-collision bifurcations and chaotic oscillations in a piecewise-smooth dynamical system," *Int. J. Bifurcation Chaos*, vol. 11, no. 12, pp. 2977–3001, 2001.

[17] R. C. Hilborn, *Chaos and Nonlinear Dynamics: An Introduction for Scientists and Engineers*. New York: Oxford Univ. Press, 2000.

[18] S. H. Strogatz, *Nonlinear Dynamics and Chaos*. Reading, MA: Addison-Wesley, 1994.

Yue Ma received the B.E. and M.E. degrees in electrical engineering from Harbin Institute of Technology, Harbin, China, and the Ph.D. degree in information systems from the University of Tokushima, Tokushima, Japan, in 1998, 2000, and 2003 respectively.

In 1999, he went to Japan as an international exchange student and began his research about nonlinear circuits, mainly bifurcation problems. From 2003 to 2004, he was a Post-Doctoral Fellow working on information optics at the Satellite Venture Business Laboratory, University of Tokushima, where, since April 2004, he is an Assistant Professor in the Department of Electrical and Electronic Engineering.

Hiroshi Kawakami (M'81) was born in Tokushima, Japan, on December 6, 1941. He received the B.Eng. degree from the University of Tokushima, Tokushima, Japan, and the M.Eng., and Dr.Eng. degrees, from Kyoto University, Kyoto, Japan, in 1964, 1966, and 1974, respectively, all in electrical engineering.

He is currently a Professor of Electrical and Electronic Engineering, and the Vice-President of the University of Tokushima. His research interest is in qualitative properties of nonlinear circuits.

Chi K. Tse (M'90–SM'97) received the B.Eng. (Hons) degree with first class honors in electrical engineering and the Ph.D. degree from the University of Melbourne, Melbourne, Australia, in 1987 and 1991, respectively.

He is currently a Professor at Hong Kong Polytechnic University, Hong Kong. His research interests include chaotic dynamics and power electronics. He is the author of *Linear Circuit Analysis* (London, U.K.: Addison-Wesley, 1998) and *Complex Behavior of Switching Power Converters* (Boca Raton, FL: CRC Press, 2003), coauthor of *Chaos-Based Digital Communication Systems* (Heidelberg, Germany: Springer-Verlag, 2003) and co-holder of a U.S. patent.

Prof. Tse was awarded the L.R. East Prize by the Institution of Engineers, Australia, in 1987, and in 2001 he won the IEEE TRANSACTIONS ON POWER ELECTRONICS Prize Paper Award. While at the University of Melbourne, he twice received the President's Award for Achievement in Research, the Faculty's Best Researcher Award and a few other teaching awards. Since 2002, he has been appointed as Guest Professor by the Southwest China Normal University, Chongqing, China. From 1999 to 2001, he served as an Associate Editor for the IEEE TRANSACTIONS ON CIRCUITS AND SYSTEMS—I: FUNDAMENTAL THEORY AND APPLICATIONS, and since 1999, he has been an Associate Editor for the IEEE TRANSACTIONS ON POWER ELECTRONICS. At present, he is also an Associate Editor for the *International Journal of Systems Science.*